Supervised Partial Volume Effect Unmixing for Brain Tumor Characterization using Multi-voxel MR Spectroscopic Imaging

Muhammad Asad [1], Guang Yang [2,3], Greg Slabaugh [1]

[1] Department of Computer Science, City University London, EC1V 0HB, London, UK
[2] Neuroscience Research Centre, St. George's, University of London, SW17 0RE, London, UK
[3] National Heart and Lung Institute, Imperial College London, SW7 2AZ, London, UK

ABSTRACT

A major challenge faced by multi-voxel Magnetic Resonance Spectroscopy (MV-MRS) imaging is partial volume effect (PVE), where signals from two or more tissue types may be mixed within a voxel. This problem arises due to the low resolution data acquisition, where the size of a voxel is kept relatively large to improve the signal to noise ratio. We propose a novel supervised Signal Mixture Model (SMM), which characterizes the MV-MRS signal into normal, low grade (infiltrative) and high grade (necrotic) brain tissue types, while accounting for in-type variation. An optimization problem is solved based on differential equations, to unmix the tissue by estimating mixture coefficients corresponding to each tissue type at each voxel. This enables visualization of probability heatmaps, useful for characterizing heterogeneous tumors. Experimental results show an overall accuracy of 91.67% and 88.89% for classifying tumors into either low or high grade against histopathology, and demonstrate the method's potential for non-invasive computer-aided diagnosis.

1. INTRODUCTION

World Health Organization guidelines classify brain tumors into four clinical grades: Grade I (GI) and II (GII) are low grade tumors that have the better prognosis and survival time, whereas Grade III (GIII) and IV (GIV) represent high grade malignant tumors [1]. Structural Magnetic Resonance Image (MRI) sequences are widely used non-invasive tools for diagnosis and grading, whereas ^{1}H Magnetic Resonance Spectroscopy (MRS) provides additional tissue metabolism information that has clinical potential to improve the non-invasive characterization of brain tumors [2].

A major challenge faced by multi-voxel Magnetic Resonance Spectroscopy (MV-MRS) imaging is the partial volume effect (PVE). PVE results in a mixture of signals from two or more tissues within a MRS voxel, which has relatively coarse resolution compared to the structural MRI in order to boost the signal to noise ratio of MV-MRS, and keep a reasonable acquisition time. Existing work using MRS for tumor type classification includes linear discriminant analysis [3], principal component analysis (PCA) and independent component analysis (ICA) [4]–[8], (convex) non-negative matrix factorization (NNMF) [9]–[12] along with multi-layered perceptron for tumor type classification. In particular, Raschke et al. was the first to address the problem of PVE with tissue type datasets, based on a technique that used LCModel and a basis set containing mean spectral representations of different tissue types, and a variability term calculated using PCA to account for tissue heterogeneity [7], [8]. Recently, Yang et al. investigated the use of nonlinear dimensionality reduction for classification of MRS tumor data [13]–[15]. Others have modeled PVE on signals in other brain image modalities for different applications [16], [17].

In this paper we propose a novel supervised Signal Mixture Model (SMM), which characterizes the MV-MRS signal into normal, low grade (infiltrative) and high grade (necrotic) brain tissue types. The proposed method is divided into training and prediction frameworks (flowchart in Figure 1). The SMM is trained using a labeled dataset of single-voxel Magnetic Resonance Spectroscopy (SV-MRS) where for each signal a single voxel is carefully placed on a homogeneous tissue region and histological tumor diagnosis is confirmed using biopsy or resected tumor tissue samples. Mean and eigenvectors encoding the variation about the mean for each tumor grade are extracted using PCA to build the SMM. The prediction stage optimizes the SMM against an input MV-MRS signal, where it addresses the PVE using mixture coefficients corresponding to each tissue type. These mixture coefficients represent the probability of each tumor grade within a given voxel, and enable visualization of probability heatmaps and identify regions of interest (ROIs) with different tumor grades. To the best of our knowledge our proposed SMM method is the first study to propose a fully supervised model for PVE estimation designed for brain tumor characterization.

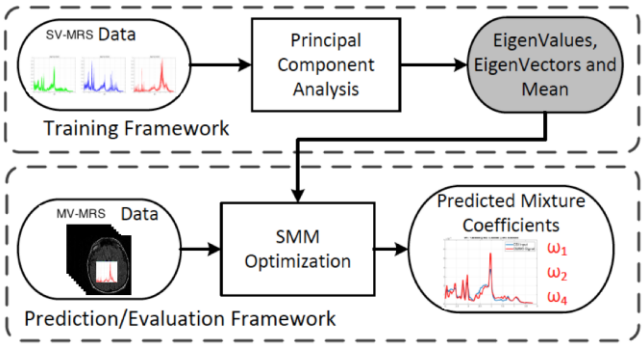

Figure 1: Flowchart of the proposed Signal Mixture Model (SMM) method.

2. SIGNAL MIXTURE MODEL FOR MV-MRS

It has been established that the tumor grade is correlated with the MRS signal, for example, a decrease in levels of N-acetylaspartate (NAA) indicates neuronal loss or damage [2]. We use this relation to propose a Signal Mixture Model (SMM) for characterizing brain tissue as Grade n, Grade l, and Grade h, corresponding to normal, low grade (infiltrative), and high grade (necrotic), respectively.

Let a MV-MRS signal be denoted as $x(t)$ and the proposed SMM denoted as $s(t)$, where x and s represent the spectrum of metabolites, and t represents the frequency in parts per million (ppm). We use a database of SV-MRS signals of each type, acquired by placing a voxel on a single homogeneous tissue region, to build signal models for each tumor grade $i \in \{n, l, h\}$. Signal models are computed using PCA to represent each signal in terms of its mean, and variation about the mean. For each grade i, we produce a model.

$$m_i(t) = \mu_i(t) + \sum_{k=1}^{K_i} \alpha_{ik}\, e_{ik}(t), \qquad (1)$$

where μ_i is the mean, e_{ik} are the eigenvectors, α_{ik} are weights that allow variation from μ_i, and K_i is the total number of selected

eigenvectors for the model. For a signal generated from a voxel that is completely from grade i, we would expect it to be well modeled with $m_i(t)$. However, particularly in MV-MRS, it is likely that the voxels will contain tissues of multiple grades due to PVE. We assume that the observed signal $x(t)$ is a mixture of $m_n(t)$, $m_l(t)$, $m_h(t)$ known as SMM, expressed as

$$s(t) = \omega_n m_n(t) + \omega_l m_l(t) + \omega_h m_h(t), \quad (2)$$

where ω_n, ω_l, ω_h are mixture coefficients that represent the probability of each tumor grade in $x(t)$ and are constrained by

$$\omega_n + \omega_l + \omega_h = 1 \text{ and } \omega_n \geq 0, \ \omega_l \geq 0, \ \omega_h \geq 0. \quad (3)$$

2.1. Signal Mixture Model (SMM) Optimization

Given a new MV-MRS signal $x(t)$, we formulate the SMM fitting as an optimization problem to determine the mixture coefficients, ω_n, ω_l, ω_h, as well as the weights α_{ik} in the model $\forall\, i$ and $\forall\, k$. This is a $(3 + K_n + K_l + K_h)$ dimensional optimization constrained by Equation 3, where our proposed method finds an optimal solution $\phi^* = [\omega\,, \omega_l^*, \omega\,, \alpha_{nk}^*, \alpha^*_{lk}, \alpha_{hk}^*] \ \forall k$. The energy to be minimized can be expressed as

$$E = \int [x(t) - s(t)]^2 dt. \quad (4)$$

To optimize this energy, we use gradient descent, which starts with an initial solution and evolves it towards an optimal solution. On each iteration η, the solution ϕ^η moves in the direction of the negative gradient, which can be derived analytically for this problem. The derivative of the energy with respect to ω_i is

$$\frac{\partial E}{\partial \omega_i} = -2 \int [\cdot] m_i(t) dt, \quad \text{where} \quad (5)$$

$$[\cdot] = x(t) - \sum_i \omega_i \left(\mu_i(t) + \sum_{k=1}^{K_i} \alpha_{ik}\, e_{ik}(t) \right). \quad (6)$$

In addition, the derivative of the energy with respect to α_{ik} is given as

$$\frac{\partial E}{\partial \alpha_{ik}} = -2 \int [\cdot] \omega_i e_{ik} dt. \quad (7)$$

We can therefore express the gradient of the energy with respect to the $(3 + 3K_n + 3K_l + 3K_h)$ parameters as

$$\nabla E = \left[\frac{\partial E}{\partial \omega_n}, \frac{\partial E}{\partial \omega_l}, \frac{\partial E}{\partial \omega_h}, \frac{\partial E}{\partial \alpha_{nk}}, \frac{\partial E}{\partial \alpha_{lk}}, \frac{\partial E}{\partial \alpha_{hk}} \right]. \quad (8)$$

2.2. Initialization and Optimization

During initialization, we take an MV-MRS signal $x(t)$ and project it into the three signal models, forming projected signals $p_i(t)$. The projection provides initial estimates for $3K_i$ weights α_{ik}.

We measure the residual r_i for each grade i, which describes the error of trying to represent signal $x(t)$ with signal model $m_i(t)$, as

$$r_i = \int [x(t) - p_i(t)]^2 dt, \quad (9)$$

If the signal is perfectly modeled using signal model $m_i(t)$, we would expect r_i to be zero. Let $r = r_n + r_l + r_h$, we initialize the mixture coefficients as

$$\omega_i = 1 - \frac{r_i}{r}, \quad (10)$$

followed by re-normalization so that they sum to one. This then gives us an initial solution ϕ^0 for SMM, as we have initial values for ω_i and α_{ik} ($\forall\, i$ and $\forall\, k$). Given the initial solution ϕ^0, we iteratively evolve the SMM in the negative gradient direction, i.e. $\phi^{\eta+1} = \phi^\eta - \gamma \nabla E^\eta$, where γ is the step size. On each iteration, we renormalize the mixture coefficients so that they are constrained by Equation 3. An example is shown in Figure 2.

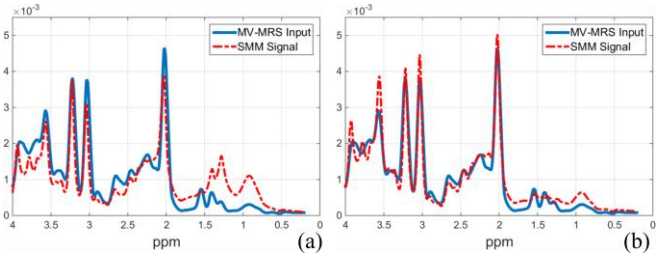

Figure 2: SMM optimization for a given input MV-MRS signal $\boldsymbol{x(t)}$ (blue). (a) SMM signal (red) for $\boldsymbol{\phi^0}$, and (b) $\boldsymbol{\phi^{10}}$.

3. EXPERIMENTAL EVALUATION

We use SV-MRS and MV-MRS datasets acquired using a GE Signa Horizon 1.5T MR system with Repetition Time (TR) = 2000 ms, short Echo Time (TE) = 30 ms. Point-resolved spectroscopic sequence and PROBE-SI protocols were used for SV-MRS and MV-MRS data acquisition, respectively. The SV-MRS data contains samples from 137 patients (79 normal, 23 GII, 10 GIII and 25 GIV). MV-MRS data was acquired from 30 patients with ground truth (GT) histological diagnosis characterizing 12 patients as GII, 7 as GIII and 11 as GIV. The SV-MRS data is used to build the SMM, where Grade n includes normal tissue samples, Grade l includes GII and Grade h includes GIV, which is then validated using MV-MRS data. Due to the heterogeneous tumor characteristics, the classification of GIII tumors can be very challenging, therefore our validation presents results including both with and without GIII data in Grade h.

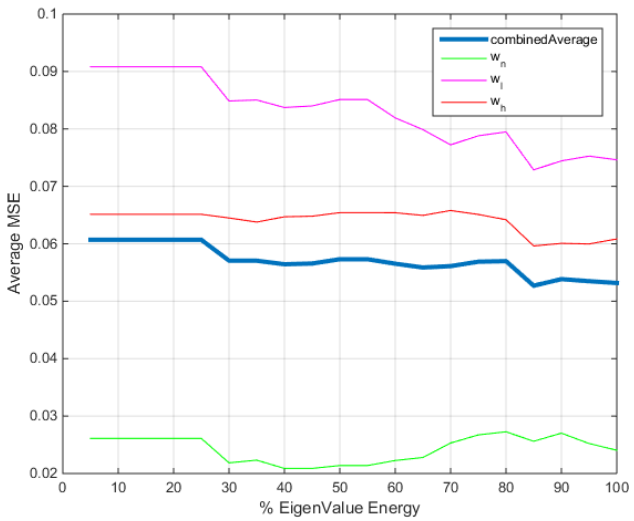

Figure 3: Cross-validation results for parameter selection shows eigenvector variation in SMM using % eigenvalue energy.

3.1. Synthetic Data Generation

Ground truth mixture coefficients for our MV-MRS data are unavailable. Therefore, we generate a synthetic MV-MRS dataset with known mixture coefficients using the SMM formed from homogeneous tissue. A sample is randomly drawn without replacement from each tumor grade $i \in \{n, l, h\}$ in SV-MRS data and used along with the GT mixture coefficients ω_{gi} covering all the possible mixture combinations to generate synthetic MV-MRS signals. The remaining SV-MRS data is used for building the proposed SMM. The whole process is repeated for 1000 iterations with each iteration having 62 possible ω_{gi} combinations for parameter selection.

3.2. Parameter Selection

The proposed SMM consists of K_i eigenvectors $e_{ik}(t)$, for $k \in \{1,2,\dots,K_i\}$, determined experimentally using cross-validation on the synthetic MV-MRS data. We vary the number of eigenvectors K_i based on the corresponding variation in % eigenvalue energy and apply SMM on synthetic MV-MRS data. Mean squared error (MSE) is calculated between estimated mixture coefficients ω_i and GT mixture coefficients $\omega_{gi}\ \forall\ i$ and MSE across all predictions for a given K_i is averaged. Figure 3 shows this MSE where it can be observed that using the 90% eigenvalue energy produces the best results. This corresponds to $K_n = 11$, $K_l = 6$ and $K_h = 3$, which we use for the rest of our experimental validation. This is due to the fact that the eigenvectors corresponding to 90% eigenvalue energy contain the most prominent signal information while filtering out the less dominant signal variations and noise.

3.3. Quantitative Validation

We compare our method with histological diagnosis for each patient in the MV-MRS data. The optimized SMM mixture coefficients ω_i are used for classifying each input sample in MV-MRS data into one of the brain tissue grades $i \in \{n, l, h\}$ by

$$i^* = \max_{i \in \{n,l,h\}} (\omega_i), \qquad (10)$$

where i^* is the predicted brain tissue class. The brain tumor is classified for a given patient as the highest grade tissue found within all MV-MRS signals for that patient. In Table 1 we compare these results with the GT histological diagnosis and present the accuracy for both the proposed SMM and the convex non-negative matrix factorization (C-NNMF) method from [10], which argues that ICA shows no advantage over C-NNMF.

Table 1: Classification accuracy using histological results as the gold standard.

Method	Grade l	Grade h		GIII Included	Overall Accuracy
	GII (12)	GIII+GIV (7+11)	GIV (11)		
C-NNMF	66.67%	83.33%	100.00%	Yes	82.93%
SMM	91.67%	88.89%	100.00%		92.68%
C-NNMF	58.33%	83.33%	100.00%	No	80.49%
SMM	91.67%	83.33%	100.00%		90.24%

From Table 1 it can be observed that the proposed SMM method produces best results when, in addition to the highest risk GIV, GIII data is also included in the Grade h training data. The proposed SMM method is able to detect GIV tumor with 100% accuracy, whereas low grade tumor and high grade tumor (GIII and GIV combined) are classified with 91.67% and 88.89% accuracy, respectively, providing promising result.

3.4. Qualitative Analysis

The estimated mixture coefficients ω_i, using the proposed SMM method, relate to the probability of classifying a given MV-MRS signal $x(t)$ into one of the three tumor grades, i.e., $i \in \{n, l, h\}$. We use these mixtures coefficients to overlay probability heatmaps for each tumor grade on the brain MRI. These results are presented along with the histological diagnosis outcome in Figure 4. Each heatmap corresponds to the probability of detection of all three tissue types, where green color represents normal grade, blue color low grade and red corresponds to high grade tumor. The 24-bit RGB representation is calculated according to the probabilities of each tissue type contributed in each MRS voxel.

4. DISCUSSION AND CONCLUSION

This paper presents a supervised learning technique that trains on ground truth data and optimizes for a given unseen signal to reliably estimate (and visualize) the relative proportion of each glioma grade in what is a relatively large MRS voxel as compared to conventional structural MRI. The SV-MRS that we used as the "ground truth" was placed according to post-Gd contrast T_1-weighted, T_2-weighted and FLAIR structural contrast on a homogenous representative tumor region with subsequent diagnosis according to clinical, radiological and histopathological information of each patient. In this study, we focused on analysis of gliomas, which are one of the more common primary brain tumor types and for which there is still a need to map out the tumor heterogeneity to aid treatment planning. There is heterogeneity of MRS characteristics within each tumor grade, and our SV-MRS data represent this, with pattern recognition applied to provide classification for MV-MRS data.

Compared to C-NNMF, our SMM method produced superior results (Table 1). This can attribute to the fact that C-NNMF is an unsupervised technique, which is suitable to cluster and map the most significant variations in the data, without any prior knowledge of the signals and hence does not incorporate for partial volume effect. In contrast to this, the proposed method is able to use an SMM, trained on SV-MRS data in a supervised fashion, to generate MV-MRS signals and reason how a given signal mixture corresponds to the variations in the input MV-MRS signal [18].

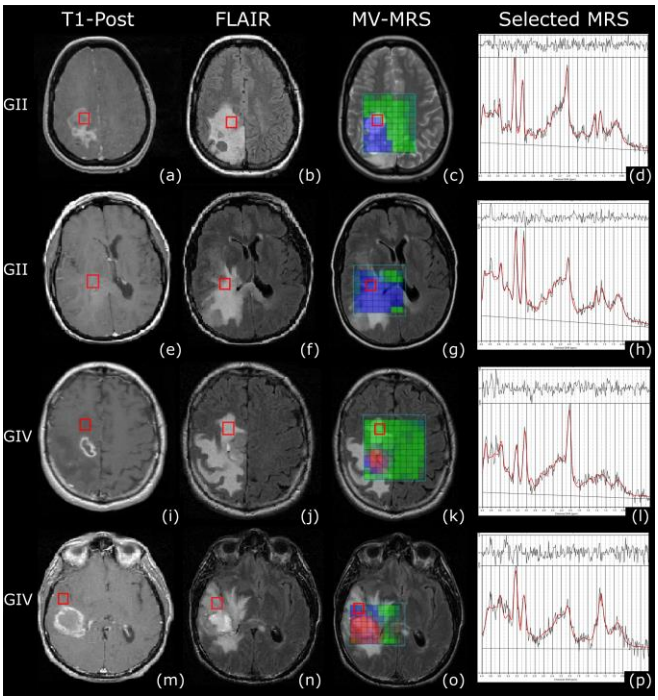

Figure 4: Example probability heatmaps and corresponding qualitative intensity based structural MR images. Selected spectra in the red boxes of each case are displayed in the last column to validate the RGB representation of the probability heatmaps.

In our method, PCA is built for each grade separately forming a model of the specific grade (normal, low grade, high grade) trained from ground truth data from SV-MRS. The tumor grade unmixing is achieved with an optimization technique using the trained models. This differs from previous unsupervised techniques where PCA (or similar methods including NNMF, ICA, and LE) of all the data is used for both clustering and unmixing the tumor grades at the same time in an essentially 'blind' fashion. A desirable feature of PCA is its ability to rank the importance of principal directions through

eigenvalue strengths. To our knowledge this optimization approach has not appeared in the literature. In addition, we avoid overfitting by selecting only the most prominent eigenvectors, ranked by eigenvalues. These selected eigenvectors capture the prominent signal variations present in the training set, while at the same time reject the intricate signal details that could result in overfitting. This selection of eigenvectors is experimentally validated (Figure 3), where one may notice overfitting with increased number of eigenvectors showing increased error.

In this study we applied the SMM on MR spectroscopic data without coupling any structural MR images because structural MRI does not always reliably describe the tumor boundary. Compared to qualitative intensities obtained using structural MRI, MRS signal directly depicts biochemistry of tumor tissue by providing relative abundance of metabolites, lipids and macromolecules. This provides a detailed biochemical representation of tissue, which may be pure tumor, normal brain tissue or a mix of both tumor and brain tissue. Although the spatial resolution of MV-MRS is not as good as structural MRI, it is well known that structural MRI cannot always detect the true extent of the tumor, whereas MV-MRS is known to provide clinically useful mapping of tumors [19]. Nevertheless, there is still a need for robust methods of analyzing MV-MRS data and its visualization for ready interpretation by radiologists in comparison to structural MRI data. Interestingly, by visually inspection of the structural MR images and comparison with the probability heatmaps generated using our SMM method, we have found vital evidence that MV-MRS can provide crucial information of tumor infiltration and extended boundaries that may not be visible in structural MR images. From a dataset of MV-MRS of glial tumors we give examples of the above points in Figure 4. Most GII tumors show no T1 post-Gd enhancement; however, in Figure 4 (a), we can see the enhanced region for this particular GII case (Figure 4 (e)-(h) shows a typical GII case). The hyper-intensity in FLAIR for GIV cases can be a mix of infiltration and oedema (Figure 4 (j)); however, in this case, the MRS spectrum shows that the FLAIR hyper-intensity region is still quite normal (Figure 4 (l)). For a region of typical GIV infiltration in the T2 hyperintensity see Figure 4 (m)-(p). Therefore, Figure 4 provides not only a qualitative visualization based validation of our probability heatmaps but also a clear demonstration that MV-MRS can catch extra critical information for tumour boundary delineation.

To summarize, we proposed a SMM based method to characterize the MV-MRS signals into normal, low grade (infiltrative) and high grade (necrotic) brain tissue types, and addressed the problem of PVE. The proposed method achieved a high accuracy of classifying tumors into either low grade or high grade while identifying high risk GIV cases with 100% accuracy. Together with the probability heatmaps overlaid on structural MRI, we can conclude that the proposed SMM based method has potential to be an alternative non-invasive tool for computer-aided brain tumor diagnosis with the far-reaching impact of surgical treatment and radiotherapy planning.

ACKNOWLEDGEMENTS

We thank Prof. Franklyn Howe and Dr. Thomas Barrick from St. George's Hospital for data and guidance. Mr. Muhammad Asad and Dr. Greg Slabaugh were supported by a City University London Pump Priming grant. Dr. Guang Yang was supported by Cancer Research UK project (Grant number: C1459/A13303). Data were acquired during projects funded by Cancer Research UK (Grant number C8807/A3870) and EU FP7 [Grant number: LSHC-CT-2004-503094 (eTUMOUR)].

5. REFERENCES

[1] D. N. Louis, H. Ohgaki, O. D. Wiestler, W. K. Cavenee, P. C. Burger, A. Jouvet, B. W. Scheithauer, and P. Kleihues, "The 2007 WHO classification of tumours of the central nervous system.," *Acta Neuropathol.*, vol. 114, no. 2, pp. 97–109, Aug. 2007.

[2] F. A. Howe and K. S. Opstad, "1H MR spectroscopy of brain tumours and masses," *NMR Biomed.*, vol. 16, no. 3, pp. 123–131, May 2003.

[3] J. Luts, T. Laudadio, A. J. Idema, A. W. Simonetti, A. Heerschap, D. Vandermeulen, J. a K. Suykens, and S. Van Huffel, "Nosologic imaging of the brain: segmentation and classification using MRI and MRSI.," *NMR Biomed.*, vol. 22, no. 4, pp. 374–90, May 2009.

[4] A. W. Simonetti, W. J. Melssen, F. Szabo de Edelenyi, J. J. a van Asten, A. Heerschap, L. M. C. Buydens, and F. S. de Edelenyi, "Combination of feature-reduced MR spectroscopic and MR imaging data for improved brain tumor classification," *NMR Biomed.*, vol. 18, no. 1, pp. 34–43, Feb. 2005.

[5] F. S. de Edelenyi, A. Simonetti, F., W. G. Postma, R. Huo, and L. M. C. Buydens, "Application of independent component analysis to 1H MR spectroscopic imaging exams of brain tumours," *Anal. Chim. Acta*, vol. 544, no. 1–2, pp. 36–46, Jul. 2005.

[6] A. J. Wright, G. Fellows, T. J. Byrnes, K. S. Opstad, D. J. O. McIntyre, J. R. Griffiths, B. a Bell, C. A. Clark, T. R. Barrick, and F. a Howe, "Pattern recognition of MRSI data shows regions of glioma growth that agree with DTI markers of brain tumor infiltration.," *Magn. Reson. Med.*, vol. 62, no. 6, pp. 1646–51, Dec. 2009.

[7] F. Raschke, G. A. Fellows, A. J. Wright, and F. A. Howe, "1H 2D MRSI tissue type analysis of gliomas.," *Magn. Reson. Med.*, vol. 73, no. 4, pp. 1381–1389, Jun. 2015.

[8] F. Raschke, "Tissue type analysis of brain tumours using multimodal MRI," St George's, University of London, 2014.

[9] S. Du, X. Mao, P. Sajda, and D. Shungu, "Automated tissue segmentation and blind recovery of 1H MRS imaging spectral patterns of normal and diseased human brain," *NMR Biomed.*, no. March 2007, pp. 33–41, 2008.

[10] S. Ortega-Martorell, P. J. G. Lisboa, A. Vellido, R. V Simões, M. Pumarola, M. Julià-Sapé, and C. Arús, "Convex non-negative matrix factorization for brain tumor delimitation from MRSI data.," *PLoS One*, vol. 7, no. 10, p. e47824, Jan. 2012.

[11] S. Ortega-Martorell, H. Ruiz, A. Vellido, I. Olier, E. Romero, M. Julià-Sapé, J. D. Martín, I. H. Jarman, C. Arús, and P. J. G. Lisboa, "A novel semi-supervised methodology for extracting tumor type-specific MRS sources in human brain data," *PLoS One*, vol. 8, no. 12, 2013.

[12] Y. Li, D. M. Sima, S. Van Cauter, A. R. Croitor Sava, U. Himmelreich, Y. Pi, and S. Van Huffel, "Hierarchical non-negative matrix factorization (hNMF): a tissue pattern differentiation method for glioblastoma multiforme diagnosis using MRSI.," *NMR Biomed.*, vol. 26, no. 3, pp. 307–19, Mar. 2013.

[13] G. Yang, F. Raschke, T. R. Barrick, and F. A. Howe, "Classification of Brain Tumour 1H MR Spectra : Extracting Features by Metabolite Quantification or Nonlinear Manifold Learning?," in *Biomedical Imaging (ISBI), 2014 IEEE 11th International Symposium on. IEEE*, 2014, pp. 1039–1042.

[14] G. Yang, F. Raschke, T. R. Barrick, and F. A. Howe, "Manifold Learning in MR Spectroscopy using Nonlinear Dimensionality Reduction and Unsupervised Clustering," *Magn. Reson. Med.*, vol. 74, no. 3, pp. 868–878, 2015.

[15] G. Yang, F. Raschke, T. R. Barrick, and F. A. Howe, "Nonlinear Laplacian Eigenmaps Dimension Reduction of in-vivo Magnetic Resonance Spectroscopic Imaging Analysis," in *International Society for Magnetic Resonance in Medicine (ISMRM)*, 2013, p. 1967.

[16] K. Van Leemput, F. Maes, D. Vandermeulen, and P. Suetens, "A unifying framework for partial volume segmentation of brain MR images," *IEEE Trans. Med. Imaging*, vol. 22, no. 1, pp. 105–119, 2003.

[17] M. Soret, S. L. Bacharach, and I. Buvat, "Partial-volume effect in PET tumor imaging.," *J. Nucl. Med.*, vol. 48, no. 6, pp. 932–945, 2007.

[18] C. M. Bishop and J. Lasserre, "Generative or discriminative? getting the best of both worlds," *Bayesian Stat.*, vol. 8, pp. 3–24, 2007.

[19] A. Pirzkall, T. R. McKnight, E. E. Graves, M. P. Carol, P. K. Sneed, W. W. Wara, S. J. Nelson, L. J. Verhey, and D. a Larson, "MR-spectroscopy guided target delineation for high-grade gliomas," *Int. J. Radiat. Oncol.*, vol. 50, no. 4, pp. 915–928, Jul. 2001.